Volatile organic compounds decomposition using nonthermal plasma coupled with a combination of catalysts

[1]*T. Zhu; [1]Y. D. Wan; [2]J. Li; [1]X. W. He; [1]D. Y. Xu; [1]X. Q. Shu; [2]W. J. Liang; [2]Y. Q. Jin

[1]*School of Chemical and Environmental Engineering, China University of Mining and Technology, Beijing, China*

[2]*College of Environmental and Energy Engineering, Beijing University of Technology, Beijing, China*

ABSTRACT: A series of experiments were performed for toluene decomposition from a gaseous influent at normal temperature and atmospheric pressure by nonthermal plasma coupled with a combination of catalysts technology. Nonthermal plasma was generated by dielectric barrier discharge. γ-Al$_2$O$_3$ was used to be a sorbent and a catalyst carrier. Nanocatalysts were MnO$_2$/γ-Al$_2$O$_3$ coupled with modified ferroelectric of nano-Ba$_{0.8}$Sr$_{0.2}$Zr$_{0.1}$Ti$_{0.9}$O$_3$. γ-Al$_2$O$_3$ played an important role in prolonging reaction time of nonthermal plasma with volatile organic compounds molecules. MnO$_2$/γ-Al$_2$O$_3$ has an advantage for ozone removal, while nano-Ba$_{0.8}$Sr$_{0.2}$Zr$_{0.1}$Ti$_{0.9}$O$_3$ is a kind of good ferroelectric material for improving energy efficiency. Thus these packed materials were incorporated together to strengthen nonthermal plasma power for volatile organic compounds decomposition. The results showed the synergistic technology resulted in greater enhancement of toluene removal and energy efficiencies and a better inhibition for ozone formation in the gas exhaust. Based on the data analysis of the Fourier transforms infrared spectrum, the reaction process of toluene decomposition and the mechanism of synergistic effect are discussed. The results showed in a complex oxidation mechanism of toluene via several pathways, producing either ringretaining or ringopening products. The final products were carbon dioxide and water.

Keywords: *Energy efficiency; Ferroelectric; Synergistic effect; Toluene*

INTRODUCTION

Volatile organic compounds (VOCs) are triggering serious environmental problems such as stratospheric ozone depletion and photochemical smog, etc. Control of VOCs in the atmosphere is a major environmental problem now and attracts more and more researchers' attentions (Futamura *et al.*, 1997; Muhamad *et al.*, 2000; Gal *et al.*, 2003; Magureanu *et al.*, 2005; Malik *et al.*, 2005; Kim, 2006; Magureanu *et al.*, 2007; Juang *et al.*, 2009a; b; Zhu *et al.*, 2009a). As one of the typical VOCs, toluene effluents came from many industries, including paints, paint thinners, fingernail polish, lacquers, adhesives, rubber and some print and leather tanning processes. Several strategies have been identified in order to reduce toluene presence in civil and industrial emissions due to its noxiousness. As an emerging technology for environmental protection, Nonthermal plasma (NTP) has been subjected to extensive researches over the past 20 years (Mizuno *et al.*, 1986; Masuda *et al.*, 1988; Chang *et al.*, 1991; Chang *et al.*, 1996; Guo *et al.*, 2006). The main advantages of NTP technology compared to the conventional technologies include moderate operation conditions (normal temperature and atmospheric pressure), moderate capital cost, compact system, easy operations and short residence times, etc. (Nunez *et al.*, 1993; Tonkyn *et al.*, 1996; Ogata *et al.*, 1999; Urashima *et al.*, 2000 ; Park *et al.*, 2003; Babel and Opiso, 2007; Subrahmanyam *et al.*, 2007).

However, the major bottleneck of developing NTP with catalysis technology is the reduction of energy consumption. If this requirement is not satisfied, the nonthermal plasma process may lose its potential for commercial applications (Yamamoto *et al.*, 1996; Tonkyn *et al.*, 2003; Young *et al.*, 2004). Many researcher found that for VOCs control, ferroelectric could improve energy efficiency significantly (Zhu *et al.*, 2011), but ozone concentration increased due to ferroelectric presence (Yamamoto *et al.*, 1992). Ogata *et al.* (2003)

✉ *Corresponding Author Email: bamboozt@cumtb.edu.cn*
Tel./Fax: +861 0623 31360

investigated the effects of alumina and metal ions in plasma discharge using NTP reactors packed with a mixture of $BaTiO_3$ and porous Al_2O_3 pellets. The results indicated that the oxidative decomposition of benzene was enhanced by concentrating benzene on the Al_2O_3 pellets. The selected catalyst of MnO_2 was well known for high potentials to decompose ozone (Van Durmea *et al*., 2007; Refaat, 2009). Futamura *et al*. (2004); Lee *et al*. (2011) and Refaat, (2011) tested catalytic effects of TiO_2 and MnO_2 with NTP. The results showed that the ozone generated from gaseous oxygen is decomposed by MnO_2, but not by TiO_2.

A series of experiments were performed for toluene decomposition from a gaseous influent at normal temperature and atmospheric pressure from 2005 to 2010 in Beijing. In this paper, the prepared nano- $Ba_{0.8}Sr_{0.2}Zr_{0.1}Ti_{0.9}O_3$ catalyst was used in the plasma reactor. Doped some ions (Sr and Zr) into the powder particles and crystal boundary in the experiment. The metal ions such as strontium, zinc and zirconium entered into crystal lattices of $BaTiO_3$ equably and the Curie temperature (Tc) fell. As a result, the permittivity of nano- $Ba_{0.8}Sr_{0.2}Zr_{0.1}Ti_{0.9}O_3$ was up to 10^4 which were 12 times higher than that of pure $BaTiO_3$, while dielectric loss reduced to 1/6 in normal temperature. This study found that this nano-material could reduce the energy consumption and increase energy efficiency significantly.

The oxidative decomposition of benzene was enhanced by concentrating toluene on the Al_2O_3 pellets. The selected catalyst of MnO_2 was well known for high potential to decompose ozone. In the experiment, the prepared MnO_2/γ-Al_2O_3 was used as catalyst to reduce

the byproducts and toluene concentrations (Zhu *et al*., 2009b) also justified about 10 wt %. The objective of this study was to use a combination of catalysts (MnO_2/γ-Al_2O_3 coupled with modified ferroelectric of nano- $Ba_{0.8}Sr_{0.2}Zr_{0.1}Ti_{0.9}O_3$) in the NTP process for toluene decomposition in order to enhance toluene decomposition efficiency and increase energy efficiency and reduce byproducts for commercial applications.

MATERIALS AND METHODS

Experimental setup

The reaction system was a tube-wire packed bed reaction system at normal temperature and atmospheric pressure. The schematic diagram of the NTP system used in this investigation is shown in Fig. 1. Dry air (78.5 % N_2, 21.5 % O_2) was used as a balance gas for toluene decomposition. Air supplied from an air compressor was divided into two air flows. Each flow rate was controlled with a mass flow meter. One air flow was introduced into a toluene liquid bottle (3) which contained liquid toluene. The air with a mass of saturated vapor of toluene was mixed with the other air flow in a blender (5) and the gaseous toluene was diluted to a prescribed concentration of 800~1000 mg/m³. A wire-tube Dielectric barrier discharge (DBD) reactor packed with catalyst was used to study the reaction as shown in Fig. 2.

An alternating current (AC) of 150 Hz was supplied to the NTP reactor in the radial direction, and the voltage extension changed from 0 kV to 50 kV. The experimental parameters of the process of discharge were detected by an oscillograph (model TDS2014, manufactured by American Tektronix Co.). The primary power values
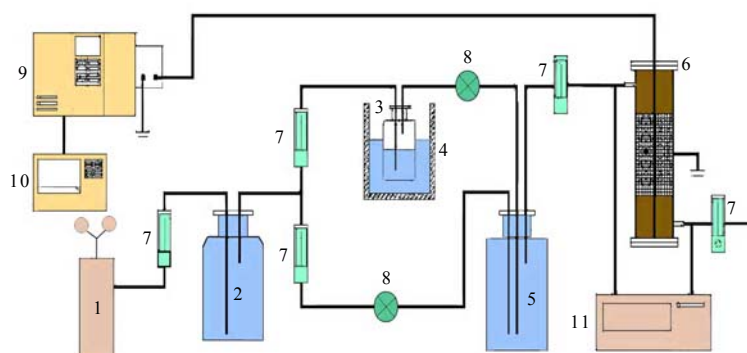
1. Air compressor 2. Buffer 3. Toluene liquid bottle 4. Attemperator 5. Blender 6. NTP reactor 7. Mass flow meter 8. Valve 9.High voltage 10. Oscillograph 11. Gas chromatography (GC)
Fig. 1: Schematic diagram of NTP system for toluene decomposition
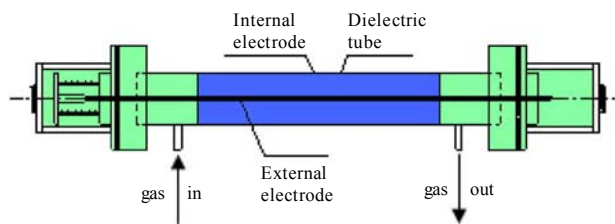
Reactor: Organic-glass tube (i.d.50 mm, length 150 mm)
Internal electrode: Tungsten filament (i.d.0.5 mm)
External electrode: Dense steel mesh

Fig. 2: NTP reactor

were measured with the voltage-charge (V-Q) Lissajous method in the plasma reactor.

Toluene decomposition was studied with a combination of catalysts including $MnO_2/\gamma-Al_2O_3$ and nano-$Ba_{0.8}Sr_{0.2}Zr_{0.1}Ti_{0.9}O_3$ catalysts (volume ratio of 1:1). The manganese oxide catalysts (5 wt %, 10 wt %, 15 wt %) were prepared by impregnation of pellet type³-alumina with the granules diameter of 5~7 mm and BET surface area of 228 m²/g detected by Micromeritics (model NOVA 1000, manufactured by American Quantachrome Co.). Nanometer - sized $Ba_{0.8}Sr_{0.2}Zr_{0.1}Ti_{0.9}O_3$ powders were prepared with inorganic salts, such as $TiCl_4$ and $Ba(OH)_2$, as the raw materials by a water-thermal method at normal pressure. Particulate diameters of $Ba_{0.8}Sr_{0.2}Zr_{0.1}Ti_{0.9}O_3$ was 59 nm which was detected by XRD (model D8 ADVANCE, manufactured by Germany Bruker Co.) and BET surface area was 8.8 m²/g. The relative permittivity of nano-$Ba_{0.8}Sr_{0.2}Zr_{0.1}Ti_{0.9}O_3$ was about 10⁴ (detected by inductance capacitance resistance (LCR) automatism test instrument 4210). The toluene concentration was determined using a gas chromatography (model HP6890N, manufactured by Agilent Co.) with a Flame ionization detector (FID) and a capillary column of HP-5 (internal diameter of 0.32 mm, length 30 m). The byproducts such as aldehyde, alcohols, amide, hydroxybenzene and polymerization products, etc, were identified by Gas chromatography mass spectrometry (GC-MS) (manufactured by American Thermo Finnegan Co.) and FT-IR (model Vertex 70, manufactured by Germany). Ozone concentration was measured by a chemical titration method of iodine (Zhu *et al.*, 2009b).

Evaluation criterion

As evaluation criterion, the toluene removal efficiency, reactor energy density and energy efficiency in the gas phase were calculated as follows.
Toluene removal efficiency (ç):

$$\eta(\%) = \frac{[toluene]_{inlet} - [toluene]_{outlet}}{[toluene]_{inlet}} \times 100\% \qquad (1)$$

Reactor input energy density (RED):

$$RED(kJ/L) = \frac{input \cdot power(W)}{gas \cdot flow \cdot rate(L/\min)} \times 60 \times 10^{-3} \qquad (2)$$

Energy efficiency (æ) :

$$\zeta(g/kWh) = \frac{[toluene]_{inlet} \times \eta}{RED} \times 3.6 \times 10^{-3} \qquad (3)$$

RESULTS AND DISCUSSION

Effect of combined catalysts on toluene removal efficiency

As the $MnO_2/\gamma-Al_2O_3$ catalyst has the best effect for ozone decomposition but not for toluene decomposition (Delagrange *et al.*, 2006) and nano-$Ba_{0.8}Sr_{0.2}Zr_{0.1}Ti_{0.9}O_3$, a type of developmental material on base of pure $BaTiO_3$ (typical ferroelectric), enhances energy efficiency because of its higher relative permittivity of 10⁴ (Shi *et al.*, 2008), a combination of nano-$Ba_{0.8}Sr_{0.2}Zr_{0.1}Ti_{0.9}O_3$ with $MnO_2/\gamma-Al_2O_3$ as a combined catalyst was tested in this study. The effect of various catalysts such as multiple catalyst, nano-$Ba_{0.8}Sr_{0.2}Zr_{0.1}Ti_{0.9}O_3$, $MnO_2/\gamma-Al_2O_3$ and no padding on removal efficiency is shown in Fig. 3 (toluene concentration: 800-1000 mg/m³; gas flow rate: 2 L/min; AC frequency: 150 Hz). The removal efficiency increased significantly with the catalysts than that without. The removal efficiency increased in the order of: combined catalyst > nano-$Ba_{0.8}Sr_{0.2}Zr_{0.1}Ti_{0.9}O_3$ > $MnO_2/\gamma-Al_2O_3$ > no padding. The best removal efficiency of 98.7 % was achieved in the NTP process. It indicated that the combination of catalysts exhibited a synergistic effect for toluene decomposition.

Effect of combined catalysts on ozone formation

Fig. 4 shows the influence of various catalysts on ozone formation with the order of: combined catalyst > MnO_2/γ-Al_2O_3 > no padding > nano-$Ba_{0.8}Sr_{0.2}Zr_{0.1}Ti_{0.9}O_3$ at RED of 0.5 kJ/L. This result suggested that MnO_2/γ-Al_2O_3 in the combination of catalysts should have a main effect on ozone decomposition.

Effect of the combination of catalysts on energy efficiency

Fig. 5 shows the influence of various catalysts on energy efficiency with the order of: combined catalyst > nano - $Ba_{0.8}Sr_{0.2}Zr_{0.1}Ti_{0.9}O_3$ > MnO_2/γ-Al_2O_3 > no padding at the same Specific discharge energy density (SED).These results indicated that the nano-$Ba_{0.8}Sr_{0.2}Zr_{0.1}Ti_{0.9}O_3$ in the combination of catalysts

should play an important role for improving energy efficiency.

As a result, the combination of catalysts shows the best removal efficiency of toluene, the best decomposition effect of ozone and the best energy efficiency for toluene removal.

Byproducts and decomposition pathways of toluene

Non-thermal plasma has high potential in air cleaning technology, but in some cases unwanted byproducts are formed which could be more harmful than the original VOCs. Fig. 6 shows the FT-IR (Fourier transforms infrared spectrum) of the byproducts of toluene decomposition and Fig. 7 shows the FT-IR spectrum of the byproducts on the surface of the combination of catalysts.
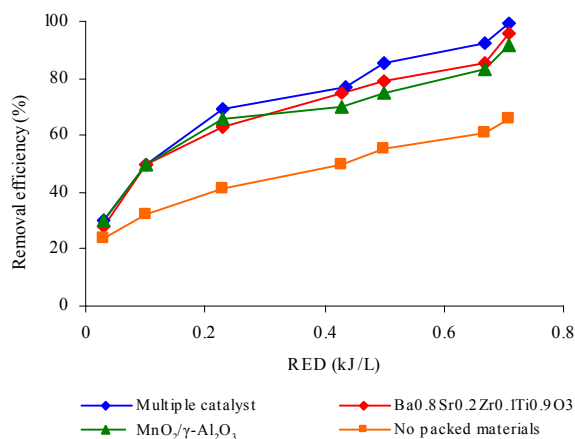

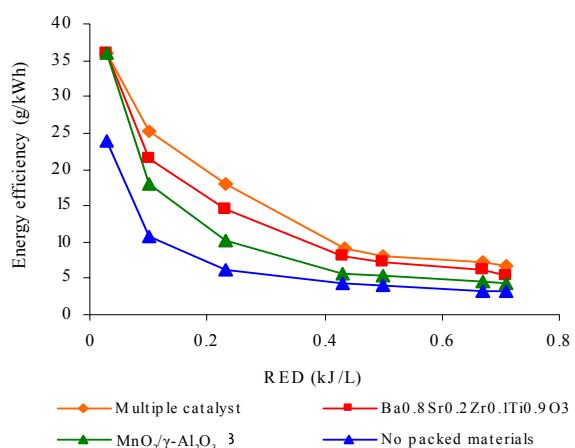Fig. 3: The change of removal efficiency with various padding

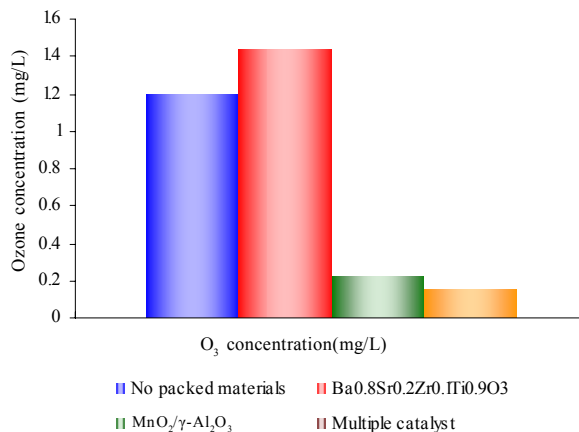Fig. 4: The change of O_3 concentration with various padding
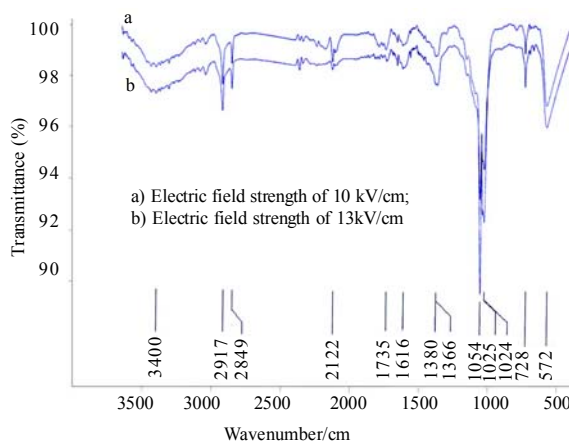

Fig. 5: The energy efficiency with various padding

Fig. 6: FT-IR spectrum of the products from toluene decomposition

624

(a) Without catalyst in the NTP reactor

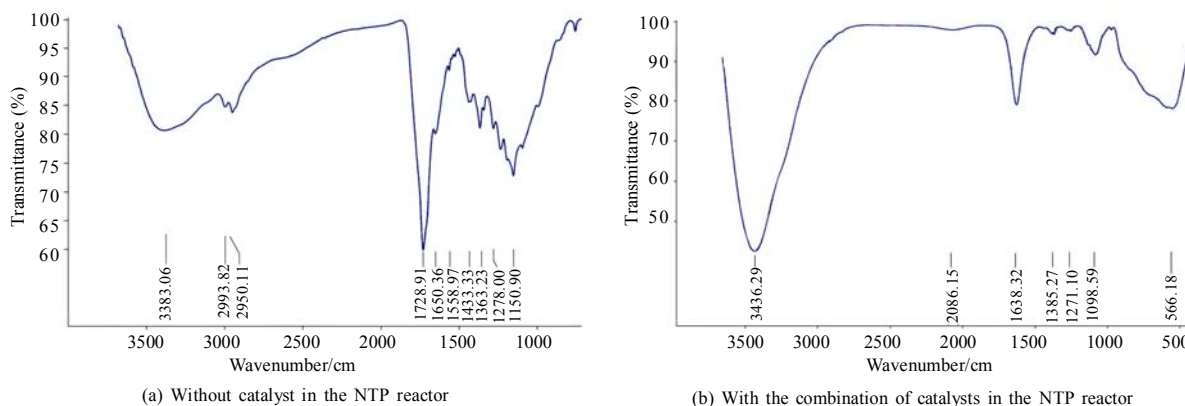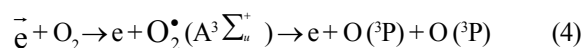(b) With the combination of catalysts in the NTP reactor

Fig. 7: FT-IR spectrum of the byproducts on the surface of the combination of catalysts

As shown in Fig. 7a, the -NH- and -NH$_2$ peak appeared at 3350/cm while the peak of 2730/cm N=C-N was absent. The peak -NH- with benzene ring appeared at 3450/cm, –OH at 3400/cm, -CH$_3$/-CH$_2$ at 2900/cm, benzene derivative (hydroxybenzene, polymerization products, etc) at 1700~1100/cm, and CO$_2$ and CO separately at the range of 2300~2100/cm and 700~500 cm^{-1} respectively. Thus, the byproducts on the surface of the combination of catalysts involved aldehyde, alcohols, amide, and benzene derivative. However, when the combination of catalysts were packed into the NTP reactor, the byproducts on the surface of the packed materials in the NTP reactor reduced greatly as shown in Fig. 7b. Except of amine, CO$_2$ and CO, no other byproducts were detected on the surface of catalysts. It illuminated that the synergic effect of the NTP with the combination of catalysts could control byproducts effectively. In Fig. 6, the products of toluene decomposition included CO$_2$, CO and H$_2$O. At the same time, there are a mass of ozone (strong peak at 1000/cm), and several amide and benzene derivatives. Compared spectrum 'a' with 'b' in Fig. 6, the benzene derivatives and ozone concentration reduce while the amounts of CO$_2$ and H$_2$O increase with the increase of the electric field strength. A large number of high-energy electrons, ions and free radicals were produced in the NTP reaction process. Firstly, the high-energy electrons could take part in reaction with oxygen in air as follow (Kim *et al.*, 2008):
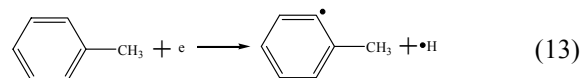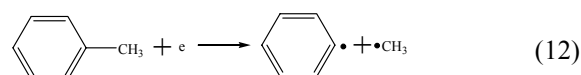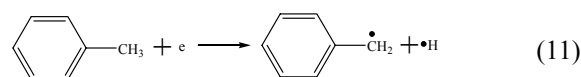
$$\vec{e} + O_2 \rightarrow e + O_2^{\bullet}(A^3\textstyle\sum_u^+) \rightarrow e + O\,(^3P) + O\,(^3P) \qquad (4)$$

$$\vec{e} + O_2 \rightarrow e + (B^3) \rightarrow e + O(^1D) + O\,(^3P) \qquad (5)$$

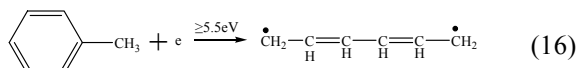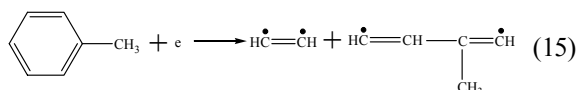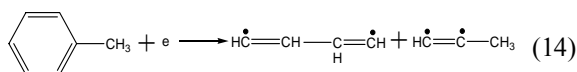The oxygen free radical groups react with oxygen and other molecules to form ozone:

$$O + O_2 + M \rightarrow O_3^{\bullet} + M \rightarrow O_3 + M \qquad (6)$$
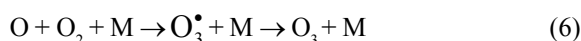
At the same time, the high-energy electrons react with H$_2$O and N$_2$ in gaseous phase:

$$e + H_2O \rightarrow OH^{\bullet} + H^{\bullet} \qquad (7)$$

$$e + H_2O \rightarrow 2H^{\bullet} + O^{\bullet} \qquad (8)$$

$$H_2O + O(^1D) \rightarrow 2OH^{\bullet} \qquad (9)$$

$$e + N_2 \rightarrow 2N^{\bullet} \qquad (10)$$

Toluene bond energy between the carbon of benzene ring and the carbon of the substituent radical is 3.6 eV, which is lower than that of carbon-carbon bond or hydrocarbon bond. As a hydrogen atom in a benzene ring is replaced by a methyl radical to form toluene, the newly formed bond is less stable and the most vulnerable. Of course, the other bonds are also likely to be destroyed by high energy electrons. Formulas 11 to 16 are the possible reaction equations of the process of toluene removal (Kohno *et al.*, 1998).

$$\text{(benzene)}-CH_3 + e \longrightarrow \text{(benzene)}-\overset{\bullet}{C}H_2 + {}^{\bullet}H \qquad (11)$$

$$\text{(benzene)}-CH_3 + e \longrightarrow \text{(benzene)}^{\bullet} + {}^{\bullet}CH_3 \qquad (12)$$

$$\text{(benzene)}-CH_3 + e \longrightarrow \text{(benzene)}^{\bullet}-CH_3 + {}^{\bullet}H \qquad (13)$$

(14)

(15)

(16)

According to the FT-IR spectrums (Fig. 7), the author speculated the reaction pathways for toluene decomposition with the NTP and the combination of catalysts (Fig. 8). The oxygen and hydroxyl free radicals of should be the inducement during the process of toluene oxidation. The oxidation process of toluene may involve many reactions and these reactions cooperate and interact with each other for toluene decomposition. Firstly, a series of chain reactions take place between OH radicals and toluene molecules due to the higher oxidation ability of OH radicals than that of oxygen radicals:

(17)

(18)

(19)
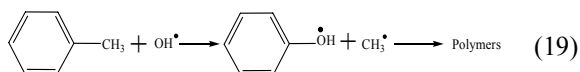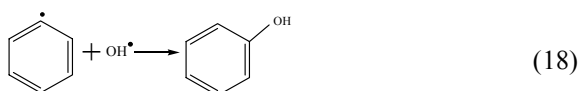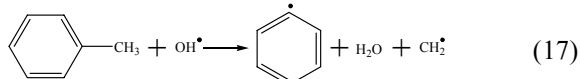
Then, the idiographic reactions occur because of oxygen free radicals during the subsequent oxidation reaction as follows:

(20)

(21)
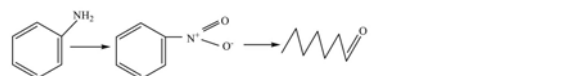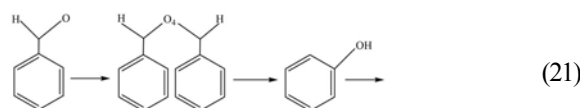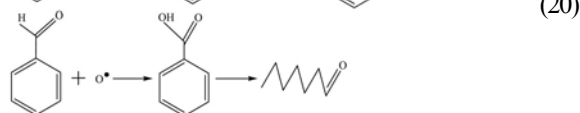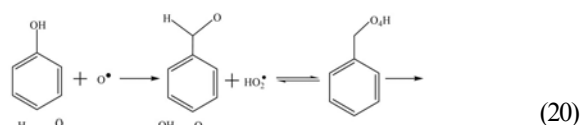
The binding bonds inside the benzene ring break down after the bonds outside the benzene ring break as follows:
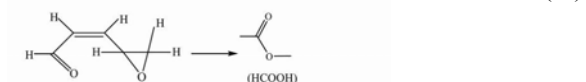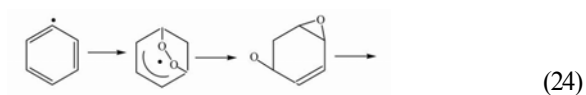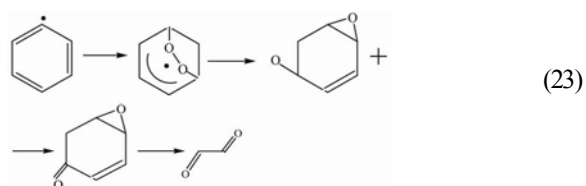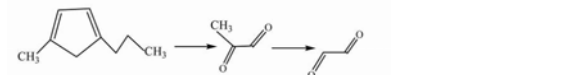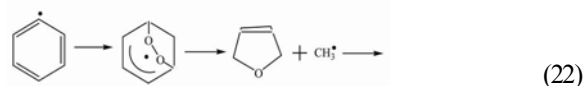
(22)

(23)

(24)

At last, the byproducts were oxidized to CO_2 and H_2O with increasing RED and the help of catalysis. At last, the byproducts were oxidized to CO_2 and H_2O with increasing RED and the help of catalysis.

(25)

(26)

(27)
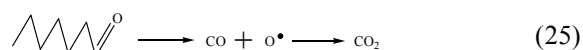
Perry *et al.* (1977) reported that aromatic compounds react with OH radicals by two pathways: hydrogen atom abstraction and OH addition to the aromatic ring. Reaction control pathways I–XII were illustrated in Fig. 8. The results showed in a complex oxidation mechanism of toluene via several pathways, producing either ring-retaining or ring-opening products. The final products were CO_2 and H_2O.

The synergistic effect of the combination of catalysts with the NTP reactor is presented in Fig. 9.

The catalyst carrier of γ-Al_2O_3 possesses sorbent characteristic, thus it could improve toluene concentration on the catalyst surface and increase the reaction time. MnO_2 is known as a metal oxide catalyst and has been reported to possess a potential activity in redox reactions. MnO_2 surface has been found to expose metal (Mn^{n+}), oxide (O^{2-}) and defect sites of various oxidation states, present degrees of coordination instauration, and exhibit acid and base properties.

Furthermore, the d–d electrons exchange interactions between intimately coupled manganese ions of different oxidation states [Mn^{n+}–O–$Mn^{(n+1)+}$] furnish the electron-mobile environment necessary for the surface redox activity (Zhu *et al.,* 2009b):

$$O_3 + Mn^{n+} \rightarrow O_2^{2-} + Mn^{(n+2)+} + O_2 \qquad (28)$$

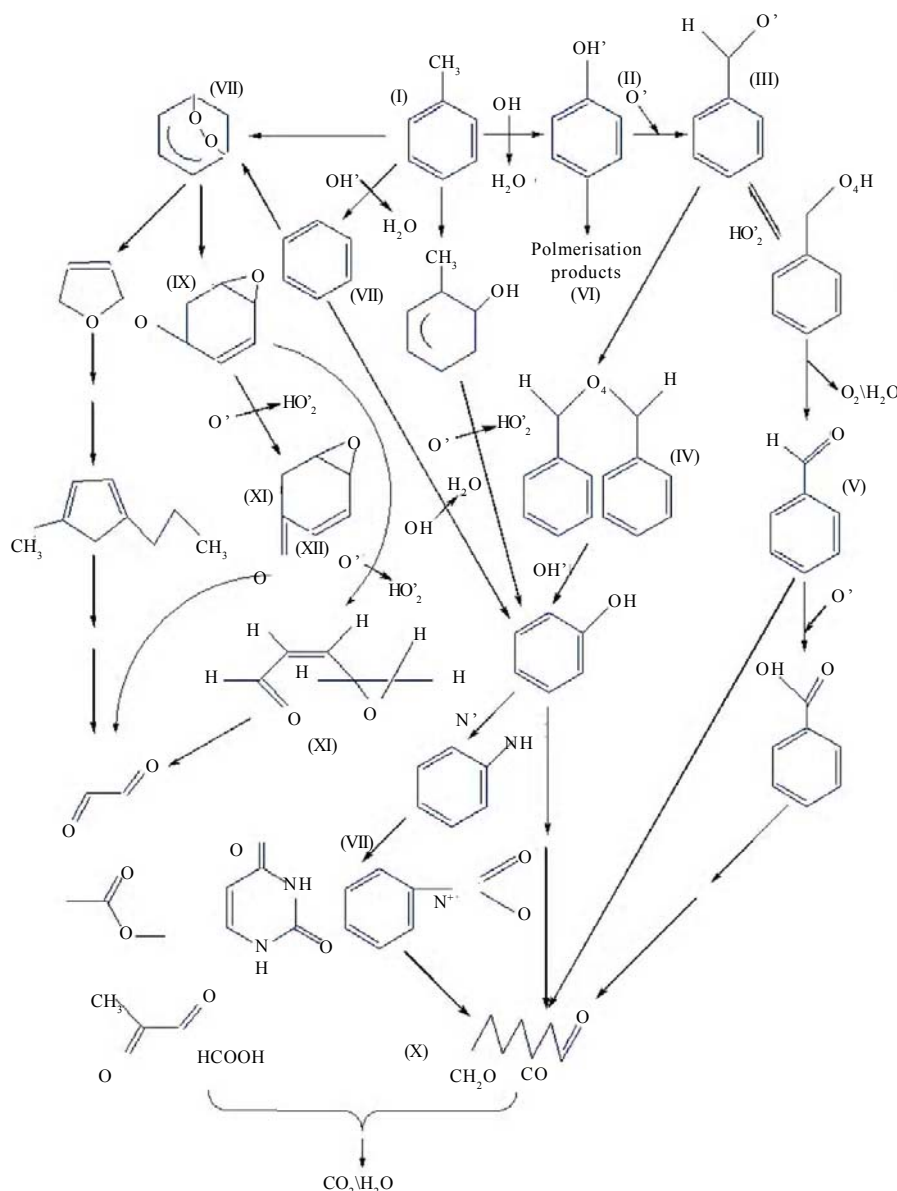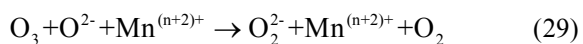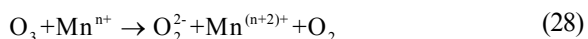$$O_3 + O^{2-} + Mn^{(n+2)+} \rightarrow O_2^{2-} + Mn^{(n+2)+} + O_2 \qquad (29)$$

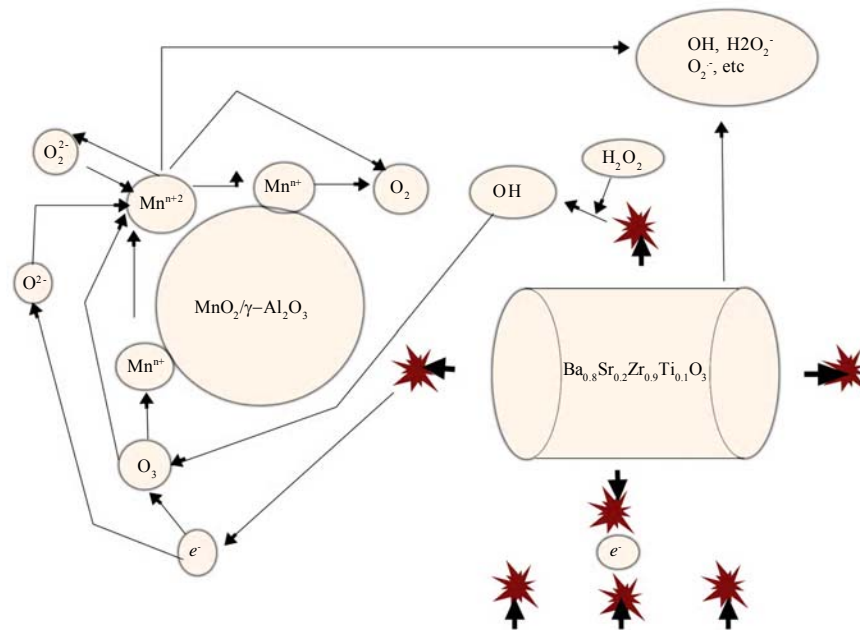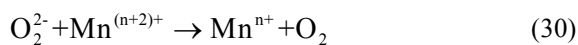Fig. 8: Abatement pathways of toluene by NTP with the combination of catalysts

Volatile organic compounds decomposition using plasma

Fig. 9: Catalysis chart of the combination of catalysts in the process of gas discharge

$$O_2^{2-}+Mn^{(n+2)+} \rightarrow Mn^{n+}+O_2 \qquad (30)$$

These factors would be helpful for toluene decomposition. Radhakrishnan (2001) reported that ozone decomposed to O^{2-} and O_2^{2-} in the surface of MnO_2. Naydenov *et al.* (1993) believed that O^- existed in the surface of MnO_2 according to the oxidation of benzene in the surface of MnO_2. As a modified ferroelectric, nano-$Ba_{0.8}Sr_{0.2}Zr_{0.1}Ti_{0.9}O_3$ has a higher dielectric constant than $BaTiO_3$ and is polarized at lower electric field strength. More high energy electrons and active radicals are generated to accelerate the reaction between NTP and toluene molecules.

CONCLUSION

Series of experiments were performed for removal of toluene gaseous influent at normal temperature and atmospheric pressure. In this study, the prepared combined catalyst was used to improve the NTP process and to take the catalytic advantages of both MnO_2/γ-Al_2O_3 and nano-$Ba_{0.8}Sr_{0.2}Zr_{0.1}Ti_{0.9}O_3$. From the view of materials application, the authors adopted NTP coupled with the combination of catalysts technology to decompose VOCs in this study. The catalyst materials could be prepared easily and inexpensing, and at the same time, this combined technology resolved the key bottlenecks effectively. Therefore, the combination of catalysts technology could advance to the NTP technology and improve applications in the industry in the future.

REFERENCES

Babel, S., Opiso, E.M., (2007). Removal of Cr from synthetic wastewater by sorption into volcanic ash soil. Int. J. Environ. Sci. Tech., 4 (1), 99-107 (**9 pages**).

Chang, M. B.; Balbach, J. H.; Rood; M. J.; Kushner, M. J., (1991). Removal of SO_2 from gas streams using a dielectric barrier discharge and combined plasma photolysis. J. Appl. Phys., 69 (8), 4409-4418 (**10 pages**).

Chang, M. B.; Tseng, T. D., (1996). Gas-phase removal of H_2S and NH_3 with dielectric barrier discharges. J. Environ. Eng., 122 (1), 41-46 (**6 pages**).

Delagrange, S.; Pinard, L.; Tatibouet, J. M., (2006). Combination of a non-thermal plasma and a catalyst for toluene removal from air: Manganese based oxide catalysts. Appl. Catal. B: Environ., 68 (3-4), 92-98 (**7 pages**).

Futamura, S.; Zhang, A. H.; Yamamoto, T., (1997). The dependence of nonthermal plasma behavior of VOCs on their chemical structures. J. Electrostat., 42 (1-2), 51-62 (**12 pages**).

Futamura, S.; Einaga, H.; Kabashima, H., (2004). Synergistic effect of silent discharge plasma and catalysts on benzene decomposition. Catal., Today, 89 (1-2), 89-95 (**7 pages**).

Gal, A.; Ogata, A.; Futamura, S., (2003). Mechanism of the dissociation of chlorofluorocarbons during nonthermal plasma processing in nitrogen at atmospheric pressure. J. Phys. Chem. A., 107 (42), 8859-8866 (**8 pages**).

Guo, Y. F.; Ye, D. Q.; Chen, K. F., (2006). Toluene decomposition using a wire-plate dielectric barrier discharge reactor with manganese oxide catalyst in situ. J. Molecular. Cata. A: Chem., 245 (1-2), 93-100 (**8 pages**).

Juang, D. F.; Lee, C. H., Hsueh, S. C., (2009a). Chlorinated volatile organic compounds found near the water surface of heavily polluted rivers. Int. J. Environ. Sci. Tech., 6 (4), 545-556 (**12 pages**).

Juang, D. F.; Yuan, C. S.; Hsueh, S. C.; Chiou, L. J., (2009b). Distribution of volatile organic compounds around a polluted river. Int. J. Environ. Sci. Tech., 6 (1), 91-104 (**14 pages**).

Kim, H. H., (2006). Effect of different catalysts on the decomposition of VOCs using flow-type plasma-driven catalysis. IEEE. Trans. Plasma. Sci., 34 (3), 984-995 (**12 pages**).

Kim, H. H.; Ogata, A.; Futamura, S., (2008). Oxygen partial pressure-dependent behavior of various catalysts for the total oxidation of VOCs using cycled system of adsorption and oxygen plasma. Appl. Catal. B: Environ., 79 (4), 356-367 (**12 pages**).

Kohno, H.; Berezin, A. A.; Chang, J. S., (1998). Destruction of volatile organic compounds used in a semiconductor industry by a capillary tube discharge reactor. IEEE. Trans. Ind. Appl., 34 (5), 953-966 (**14 pages**).

Lee, K.; Lee, E.; Lee, H.; Kim, Y. K.; Sohn, K., (2011). Hydrogen peroxide interference in chemical oxygen demand during ozone based advanced oxidation of anaerobically digested livestock wastewater. Int. J. Environ. Sci. Tech., 8 (2), 381-388 (**8 pages**).

Magureanu, M.; Mandache, N. B.; Hu, J. C.; Richards, R.; Florea, M.; Parvulescu, V. I., (2005). Plasma-assisted catalysis for volatile organic compounds abatement. Appli. Cata. B: Environ., 61 (1-2), 12-20 (**9 pages**).

Magureanu, M.; Mandache; N. B.; Parvulescu, V. I.; Subrahmanyam, C.; Renken, A.; Kiwi Minsker, L., (2007). Improved performance of non-thermal plasma reactor during decomposition of trichloroethylene: Optimization of the reactor geometry and introduction of catalytic electrode. Appl. Catal. B: Environ., 74 (3-4), 270-277 (**8 pages**).

Malik, M. A.; Minamitani, Y.; Schoenbach, K. H., (2005). Comparison of catalytic activity of aluminum oxide and silica gel for decomposition of volatile organic compounds (VOCs) in a plasmacatalytic reactor. IEEE. Trans. Plasma. Sci., 33 (1), 50-56 (**7 pages**).

Masuda, S., (1988). Pulse corona induced plasma chemical process: a horizon of new plasma chemical technologies. Pure. Appl. Chem., 60 (5), 727-731 (**5 pages**).

Mizuno, A.; Clements, J. S.; Davis. R. H., (1986). A method for the removal of sulfur dioxide from exhaust gas utilizing pulsed streamer corona for electron energization. IEEE. Trans. Ind. Appl., 22 (3), 516-522 (**7 pages**).

Muhamad. A. M.; Jiang. X. Z., (2000). Catalyst assisted destruction of trichloro ethylene and toluene in corona discharges. J. Environ. Sci., 12 (1), 7-11 (**5 pages**).

Naydenov, A.; Mehandjiev. D., (1993). Complete oxidation of benzene on manganese dioxide by ozone. App1.Cata1. A: Gen., 97 (1), 17-22 (**6 pages**).

Nunez, C. M.; Ramsey. G. H.; Ponder, W. H.; Abbott, J. H.; Hamel, L. E.; Kariher, P. H., (1993). Corona destruction: An innovative control technology for VOCs and air toxics. Air. Waste., 43 (2), 242-247 (**6 pages**).

Ogata, A.; Einaga, H.; Kabashima, H., (2003). Effective combination of nonthermal plasma and catalysts for decomposition of benzene in air. Appl. Catal. B: Environ., 46 (1), 87-95 (**9 pages**).

Ogata, A.; Yamanonchi, K.; Mizuno, K., (1999). Decomposition of benzene using alumina-hybrid and catalyst-hybrid plasma reactors. IEEE. Trans. Ind. Appl., 35 (6), 1289-1295 (**7 pages**).

Park, J. Y.; Jung, J. G.; Kim, J. S., (2003). Effect of nonthermal plasma reactor for CF decomposition. IEEE. Trans. Plasma. Sci., 31 (6), 1349-1354 (**6 pages**).

Perry, R. A.; Atkinson, R.; Pitts, J. N., (1977). Kinetics and mechanism of the gas phase reaction of hydroxyl radicals with aromatic hydrocarbons over the temperature range 296-473 K. J. Phys. Chem., 81 (4), 296-304 (**9 pages**).

Radhakrishnan, R.; Oyama, S. T.; Chen, J. G., (2001). Electron transfer effects in ozone decomposition on supported manganese oxide. J. Phys. Chem. B., 105 (19), 4245-4253 (**9 pages**).

Refaat, A. A. (2009). Correlation between the chemical structure of biodiesel and its physical properties. Int. J. Environ. Sci.Tech., 6 (4), 677-694 (**8 pages**).

Refaat, A. A., (2011). Biodiesel production using solid metal oxide catalysts. Int. J. Environ. Sci. Tech., 8 (1), 203-221 (**19 pages**).

Shi, A. H., Yan, W. B., Li, Y. J.; Huang, K. L., (2008). Preparation and characterization of nanometer-sized barium titanate powder by complex-precursor method. J.Centr. South Univ. Tech., 15 (3), 224-228 (**5 pages**).

Subrahmanyam, C.; Renken, A.; Kiwi-Minsker, L., (2007). Novel catalytic non-thermal plasma reactor for the abatement of VOCs. Chem. Eng. J., 134 (1-3), 78-83 (**6 pages**).

Tonkyn, R. G.; Barlow, S. E.; Orlando, T. M., (1996). Destruction of carbon tetrachloride in a dielectric barrier/ packed-bed corona reactor. J. Appl. Phys., 80 (9), 4877-4886 (**10 pages**).

Tonkyn, R. G.; Barlow, S. E.; Hoard, J., (2003). Reduction of NOx in synthetic diesel exhaust via two-step plasma-catalytic treatment. Appl. Catal. B. Environ., 40 (3), 207-217 (**11 pages**).

Urashima, K.; Chang, J., (2000). Removal of volatile organic compounds from air streams and industrial flue gases by non-thermal plasma technology. IEEE. Trans. Dielectr. Electr. Insul., 7 (5), 602-614 (**13 pages**).

Van Durmea, J.; Dewulfa, J.; Sysmansa, W.; Leysb, C.; Van Langenhove, H., (2007). Efficient toluene abatement in

indoor air by a plasma catalytic hybrid system. Appl. Cata. B: Environ., 74 (1-2), 161-166 (**6 pages**).

Yamamoto, T.; Ramanatiran, K.; Lawless, P. A.; Ensor, D. S.; Nwesome, J. R.; Plaks, N.; Ramsey, G. H., (1992). Control of Volatile organic compound by ac energized ferroelectric pellet reactor and a pulsed corona reactor. IEEE Trans. Ind. Appl., 28 (3), 528-533 (**6 pages**).

Yamamoto, T.; Mizuno, K.; Tamori, I.; Ogata, A.; Nifuku, M.; Michalska, M.; Prieto, G., (1996). Catalysis-assisted plasma technology for carbon tetrachloride destruction. IEEE. Trans. Ind. Appl., 32(1), 100-106 (**7 pages**).

Young, S. M.; Dors, M.; Jerzy, M., (2004). Effect of reaction temperature on NOx removal and formation of ammonium nitrate in nonthermal plasma process combined with selective catalytic reduction. IEEE. Trans. Plasma. Sci., 32 (1), 799-807 (**9 pages**).

Zhu, T. ; Li, J.; Jin, Y. Q.; Liang, Y. H.; Ma, G. D., (2009a). Gaseous phase benzene decomposition by nonthermal plasma coupled with nano-titania catalyst. Int. J. Environ. Sci. Tech., 6 (1), 141-152 (**12 pages**).

Zhu, T. ; Li, J. ; Liang, W. J.; Jin, Y. Q., (2009b). Synergistic effect of catalyst for oxidation removal of toluene. J. Hazard. Mater., 165, 1258-1261 (**4 pages**).

Zhu, T.; Wan, Y. D.; He, X. W.; Xu, D. Y.; Shu, X. Q., (2011). Effect of modified ferroelectric on nonthermal plasma process for toluene decomposition. Fresen. Environ. Bull., 20 (1), 149-155 (**7 pages**).

AUTHOR (S) BIOSKETCHES

Zhu, T., Ph.D., School of Chemical and Environmental Engineering, China University of Mining and Technology, Ding No.11, Xueyuan Rode, Haidian District, Beijing 100083, China. Email: *bamboozt@cumtb.edu.cn*

Wan, Y. D., M.Sc., School of Chemical and Environmental Engineering, China University of Mining and Technology, Ding No.11, Xueyuan Rode, Haidian District, Beijing 100083, China. Email: *bamboozt@sohu.com*

Li, J., Ph.D., Professor, College of Environmental and Energy Engineering, Beijing University of Technology, 100# Ping Leyuan, Chaoyang District, Beijing 100124, China. E-mail: *ljian@bjtu.edu.cn*

He, X. W., Ph.D., Professor, School of Chemical and Environmental Engineering, China University of Mining and Technology. Ding No.11, Xueyuan Rode, Haidian District, Beijing 100083, China. Email: *hjinghua@vip.sina.com*

Xu, D. Y., Ph.D., Professor, School of Chemical and Environmental Engineering, China University of Mining and Technology, Ding No.11, Xueyuan Rode, Haidian District, Beijing 100083, China. Email: *xudongyao101@163.com*

Shu, X. Q., Ph.D., Professor, School of Chemical and Environmental Engineering, China University of Mining and Technology, Ding No.11, Xueyuan Rode, Haidian District, Beijing 100083, China. Email: *xqshu@cumtb.edu.cn*

Liang, W. J., Ph.D., Associate Professor, College of Environmental and Energy Engineering, Beijing University of Technology. 100# Ping Leyuan, Chaoyang District, Beijing 100124, China. Email: *lwj@bjut.edu.cn*

Jin, Y. Q., Ph.D., Professor, College of Environmental and Energy Engineering, Beijing University of Technology. 100# Ping Leyuan, Chaoyang District, Beijing 100124, China. Email: *jyq@bjut.edu.cn*

www.SID